# THSD1 preserves vascular integrity and protects against intraplaque haemorrhaging in ApoE(-/-) mice

Cardiovascular Research (2016) **110**, 129–139
doi:10.1093/cvr/cvw015

# *THSD1* preserves vascular integrity and protects against intraplaque haemorrhaging in ApoE$^{-/-}$ mice

**Remco A. Haasdijk[1†], Wijnand K. Den Dekker[1†], Caroline Cheng[1,2†], Dennie Tempel[3‡], Robert Szulcek[4‡], Frank L. Bos[1,5‡], Dorien M.A. Hermkens[1,5‡], Ihsan Chrifi[1,2], Maarten M. Brandt[1,2], Chris Van Dijk[2], Yan Juan Xu[2], Esther H.M. Van De Kamp[1], Lau A.J. Blonden[1], Jan Van Bezu[4], Judith C. Sluimer[6], Erik A.L. Biessen[6], Geerten P. Van Nieuw Amerongen[4], and Henricus J. Duckers[3]***

[1]Department of Cardiology, Erasmus Medical Center Rotterdam, Rotterdam, The Netherlands; [2]Regenerative Vascular Medicine Laboratory, Department of Nephrology and Hypertension, Division of Internal Medicine and Dermatology, University Medical Center Utrecht, Heidelberglaan 100, PO Box 85500, 3584 CX Utrecht, 3508 GA Utrecht, The Netherlands; [3]Department of Cardiology, University Medical Center Utrecht, Utrecht, The Netherlands; [4]Department of Physiology, Institute for Cardiovascular Research, VU University Medical Center Amsterdam, Amsterdam, The Netherlands; [5]Hubrecht Institute, Utrecht, The Netherlands; and [6]Department of Pathology, Maastricht University Medical Center, Maastricht, The Netherlands

*Received 16 June 2015; revised 30 December 2015; accepted 7 January 2016; online publish-ahead-of-print 27 January 2016*

**Time for primary review: 29 days**

**Aims** Impairment of the endothelial barrier leads to microvascular breakdown in cardiovascular disease and is involved in intraplaque haemorrhaging and the progression of advanced atherosclerotic lesions that are vulnerable to rupture. The exact mechanism that regulates vascular integrity requires further definition. Using a microarray screen for angiogenesis-associated genes during murine embryogenesis, we identified thrombospondin type I domain 1 (*THSD1*) as a new putative angiopotent factor with unknown biological function. We sought to characterize the role of *THSD1* in endothelial cells during vascular development and cardiovascular disease.

**Methods and results** Functional knockdown of *Thsd1* in zebrafish embryos and in a murine retina vascularization model induced severe haemorrhaging without affecting neovascular growth. In human carotid endarterectomy specimens, *THSD1* expression by endothelial cells was detected in advanced atherosclerotic lesions with intraplaque haemorrhaging, but was absent in stable lesions, implying involvement of *THSD1* in neovascular bleeding. *In vitro*, stimulation with pro-atherogenic factors (3% $O_2$ and TNFα) decreased *THSD1* expression in human endothelial cells, whereas stimulation with an anti-atherogenic factor (IL10) showed opposite effect. Therapeutic evaluation in a murine advanced atherosclerosis model showed that *Thsd1* overexpression decreased plaque vulnerability by attenuating intraplaque vascular leakage, subsequently reducing macrophage accumulation and necrotic core size. Mechanistic studies in human endothelial cells demonstrated that THSD1 activates FAK-PI3K, leading to Rac1-mediated actin cytoskeleton regulation of adherens junctions and focal adhesion assembly.

**Conclusion** *THSD1* is a new regulator of endothelial barrier function during vascular development and protects intraplaque microvessels against haemorrhaging in advanced atherosclerotic lesions.

**Keywords** Vulnerable plaque • Intraplaque haemorrhage • Endothelial function • *THSD1*

## 1. Introduction

Vascular barrier integrity of the endothelium is actively controlled by dynamic interactions between the endothelial actin cytoskeleton, cell-to-cell junctions, and cell-to-extracellular matrix (ECM) focal adhesion contacts.[1,2] Loss of barrier function leads to passage of circulating cells and solutes and contributes to (micro)vascular haemorrhaging. Although intercellular contacts are established between endothelial cells during the earliest phases of vasculogenesis and angiogenesis, a functional barrier is only created after the critical process of

* Corresponding author. Tel: +31 88 7556167; fax: +31 88 7551750, E-mail: h.j.duckers@umcutrecht.nl

† These authors contributed equally.

‡ These authors contributed equally.

junction maturation that is stringently controlled by members of the Rho family of GTPases.[3–6] In particular, Rac1 regulation of actin cytoskeleton dynamics prevents the build-up of actomyosin-mediated tension across VE-cadherin adhesion sites, which is crucial for the formation of stable adherens junctions that provide the mechanical cohesion of the intercellular bonds.[7] Disruption of the Rac1 regulatory pathway leads to loss of vascular integrity and is implicated to be an important contributing factor to vascular-related diseases, including atherosclerosis.[1,8]

In advanced atherosclerosis, lesions become characterized by intraplaque growth of microvessels that are phenotypically immature and are defined by lack of endothelial barrier function, making them susceptible to haemorrhaging and rupture.[9] Although the importance of loss of barrier integrity in the onset of cardiovascular disease has become increasingly evident, our knowledge of endothelial specific factors that orchestrate the key Rac1-mediated pathway in vascular barrier regulation remains limited. In this study, we report a new gene with a high level of endothelial specific expression that is a potent preservation factor of vascular barrier integrity.

Recently, we have carried out a genome-wide microarray analysis in search for genes involved in the regulation of new vessel formation and have identified thrombospondin type I domain 1 (*THSD1*), also known as transmembrane molecule with thrombospondin module (*TMTSP*), as a new candidate regulator of vascular development. *THSD1* has been described as an early marker of haematopoietic stem cells and ECs during embryonic development in mice.[10] *In silico* database analysis indicated that *THSD1* encodes for a putative protein structure that contains a signal sequence and a transmembrane and thrombospondin type 1 repeat (TSP1) domain. Currently, data that elucidate the vascular function of THSD1 are still lacking.

Here, we sought to characterize the function of THSD1 in ECs during blood vessel formation *in vitro*, using primary cell cultures, and *in vivo* in zebrafish and murine vascular development. Our studies identified, for the first time, THSD1 as a critical regulator of Rac1-mediated conservation of neovessel integrity. *Thsd1* knockdown induced microvascular ruptures and haemorrhaging during embryonic and postnatal vascular development, indicating that THSD1 is a beneficial factor for maintaining endothelial barrier function. The therapeutic potential of THSD1 was investigated in our well-validated murine ApoE-knockout model in which we induced growth of vulnerable plaque-like lesions by shear stress alteration.[11,12] *Thsd1* overexpression improved endothelial barrier function and reduced vascular bleeding of the neointimal microvasculature in the murine atherosclerotic plaques. Considering the potent vascular stabilizing function of the gene, we propose that *THSD1* is an interesting drug target for the development of therapeutics in the treatment of vulnerable plaque or other (micro)vascular pathologies in which endothelial barrier function is compromised.

# 2. Methods

## 2.1 Ethics

The human samples were obtained from the Maastricht Pathology Tissue collection bank (MPTC). Collection and storage in the MPTC and patient data confidentiality as well as tissue usage were in accordance with the 'Code for Proper Secondary Use of Human Tissue in the Netherlands' (http://www.fmwv.nl, http://www.federa.org/sites/default/files/digital_version_first_part_code_of_conduct_in_uk_2011_12092012.pdf). Collection and study of human samples were approved by institutional ethics committee and have been performed in full accordance with the ethical standards laid down in the 1964 Declaration of Helsinki and its later amendments. All animal studies were carried out in accordance with the Council of Europe Convention Directive (2010/63/EU) for the protection of vertebrate animals used for experimental and other scientific purposes with the approval of the National and Local Animal Care Committee.

## 2.2 Mouse model of retinal vascularization

Two-day-old murine C57BL/6J male and female pups were anaesthetized by placement on ice. One microlitre of *Thsd1* targeting siRNA (1.33 μg/μL) was injected into the left eye using a 33-Gauge needle (World Precision Instruments, Berlin, Germany). As control, one microlitre of scrambled non-targeting siRNA (1.33 μg/μL) was injected into the right eye. SiRNA was obtained from Thermo Fisher Scientific (Breda, The Netherlands). The following mix of mouse *Thsd1* targeting siRNA was used: 5′-GCA AGC AAG UUC CGA AUC A-3′, 5′-AGU CAU UGC UUC UAC GGG A-3′, 5′-GCU CCA ACG AAG AGG ACG A-3′, 5′-UGA CUA UGU CCU CGG AGA A-3′. Mice pups were killed 5 days after intraocular injection by decapitation. The retinas were stained with Alexa Fluor® 488-conjugated isolectin GS-$IB_4$ 1:200 (I21411; Invitrogen, Bleiswijk, The Netherlands) before assessment under a fluorescence microscope (Axiovert S100; Carl Zeiss, Sliedrecht, The Netherlands). Image analysis of number of junctions, tubules, and total tubule length was carried out using Angiosys Image Analysis Software 1.0 (TCS CellWorks, Buckingham, UK). Validation of adequate *Thsd1* knockdown in the retina (2 days after intra-ocular injection) was achieved by qPCR using the following mouse primers: 5′-AGA GCC AGC AAA AGG ACA AA-3′ (forward) and 5′-CAA GGA GGT GGC AGT ACC AT-3′ (reverse) (Biolegio, Nijmegen, The Netherlands). HPRT primers 5′-TCA GGA GAG AGA AAA GAT GTG ATT GA-3′ (forward) and 5′-ACG CCA ACA CTGCTG AAA CA-3′ (reverse) (Biolegio, Nijmegen, The Netherlands) were used for housekeeping gene detection.

## 2.3 ApoE-knockout mice vulnerable plaque model

Ten-week-old female $ApoE^{-/-}$/C57BL/J6 mice (Jackson Laboratory, UK) were put on a Western diet containing 15% (w/w) cacao and 0.25% (w/w) cholesterol (Arie Blok, Woerden, The Netherlands). Two weeks after start of the Western diet, mice were anaesthetized by ventilation of a 1:2 mixture of $O_2$/$N_2O$ to which 2.3% isoflurane was added. The animals were maintained at 37°C on a heating pad during the operation; a neck incision was made and the right common carotid artery was dissected from connective tissue. A tapered cast was surgically implanted around the right common carotid artery. This device reduces flow shear stress upstream, triggering the growth of atherosclerotic lesions with a vulnerable plaque phenotype. Nine weeks after cast placement, mice were re-operated and locally transfected with either adenovirus-expressing murine Thsd1 or sham virus. At Day 5, 1 h before sacrifice by cervical dislocation, FITC-labelled dextran (Sigma-Aldrich, Zwijndrecht, The Netherlands) was intravenously injected. The carotid artery was flushed and harvested. The carotids that were treated with the shear stress altering device were cut at the proximal and distal borders of the cast to separate the blood vessel into three different segments: Section 1, segment proximal from device (the vulnerable plaque section); Section 2, a segment distal from the device (the stable plaque section); and Section 3, a segment of the carotid that was encased by the device and which was discarded. Section 1 (proximal) and Section 2 (distal) were used for qPCR analysis of the vulnerable plaque and stable lesion area, respectively.

A more detailed description of all methods is available in the Supplementary material online.

# 3. Results

## 3.1 Vascular-specific mRNA expression of *Thsd1* during mouse development

To identify new gene targets involved in angiogenesis, mRNA expression profiles of Flk1-positive angioblasts separated by flow cytometric sorting at various stages of murine embryonic development were compared with Flk1-negative cells. *Thsd1* was up-regulated in Flk1-positive angioblasts from 8 to 16 days post-fertilization. Expression levels peaked from 8 to 11 days post-fertilization, which coincided with the period of early angiogenesis in murine development (*Figure 1A*).

## 3.2 Vascular-specific mRNA expression of *Thsd1* during zebrafish development

In line with the findings from murine embryos indicating that *thsd1* is mainly expressed in the endothelial cell lineage, whole-mount *in situ* hybridization in developing zebrafish larvae showed expression of the *thsd1* zebrafish orthologue in the main axial vessels (dorsal aorta and posterior cardinal vein) and head vessels at 26 h post-fertilization. In addition, *thsd1* expression was also detected in the caudal and mid-cerebral veins, and in the somites (*Figure 1B*).

## 3.3 Knockdown of *thsd1* in zebrafish induces haemorrhaging of cerebral vessels

For functional evaluation of *thsd1 in vivo*, the gene was silenced in developing zebrafish larvae of the transgenic zebrafish lines Tg(fli1:eGFP)$^{y1}$ and Tg(kdrl:eGFP x gata1:dsRed)$^{y1}$, using morpholino (MO) knockdown technology. Successful targeting of *thsd1* was verified by qPCR analysis (see Supplementary material online, *Figure S1*). Silencing of *thsd1* had no effect on vascular growth (*Figure 2A*). However, time-lapse studies carried out during the first 48 h post-fertilization identified severe and frequent haemorrhaging in the cranial region, a known predilection site for vascular haemorrhaging in zebrafish,[13,14] which was observed in 24% of the injected embryos ($n = 195$) (*Figure 2B–E*). Haemorrhaging occurred as a sudden rupture of blood vessels, implying intrinsic weakness and lack of integrity of the endothelial barrier (*Figure 2B* and *C*). Cerebral haemorrhaging was further confirmed by an *o*-Dianisidine staining of iron/heme in red blood cells in *thsd1*-silenced wild-type zebrafish (*Figure 2D*). This phenotype was consistently observed in the *thsd1*-silenced zebrafish after injections of different MO concentrations (*Figure 2E*).

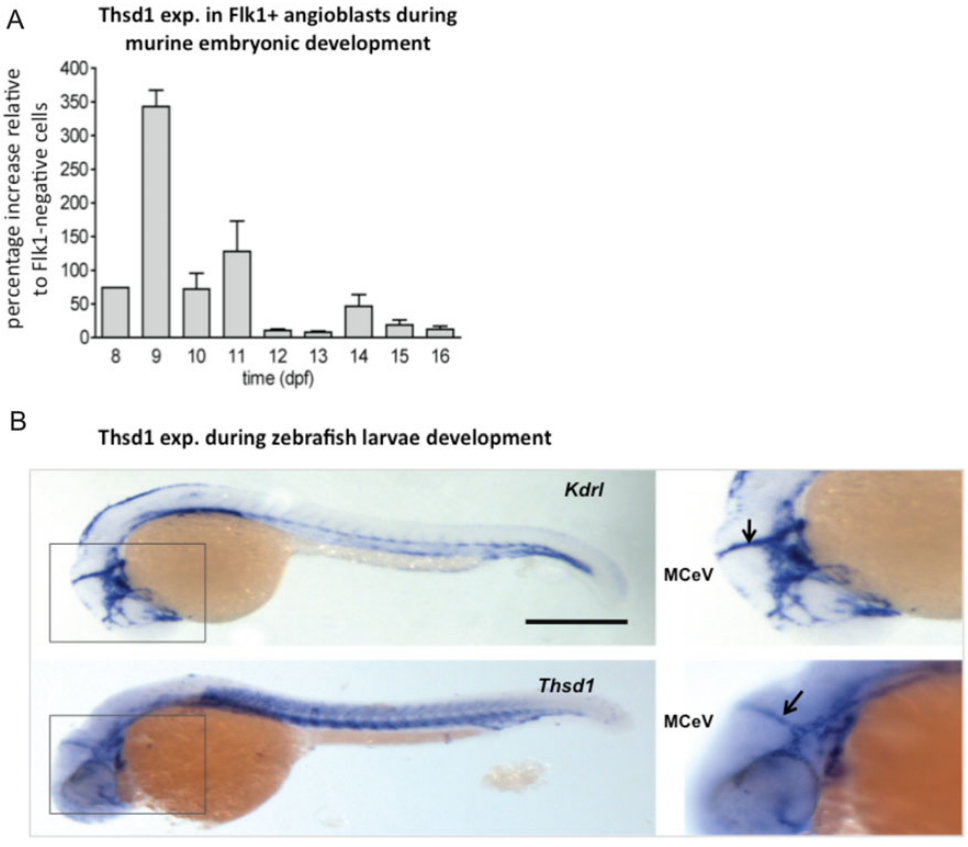


**Figure 1** Vascular-specific expression of *Thsd1* during mouse and zebrafish development. (*A*) Endogenous expression level of *Thsd1* in Flk1-positive angioblasts during murine embryonic development from 8 to 16 days post-fertilization (dpf) vs. Flk1-negative cells, analysed by qPCR. *Thsd1* mRNA level in Flk1-negative cells was set to baseline ($n = 4$; mean ± SEM). (*B*) Whole-mount *in situ* hybridization comparison of endothelial specific kdrl (upper panel) with *thsd1* (lower panel) in zebrafish at 26 h post-fertilization (hpf), lateral view, anterior to the left. Like kdrl, *thsd1* transcripts were localized in the developing vascular network, including the cerebral vasculature [indicated by black arrows are the caudal and mid-cerebral veins (MCeV)]. In addition, expression of *thsd1* in the somites was observed. Right-hand panel shows high magnification images of the head region. Scale bar = 200 μm.

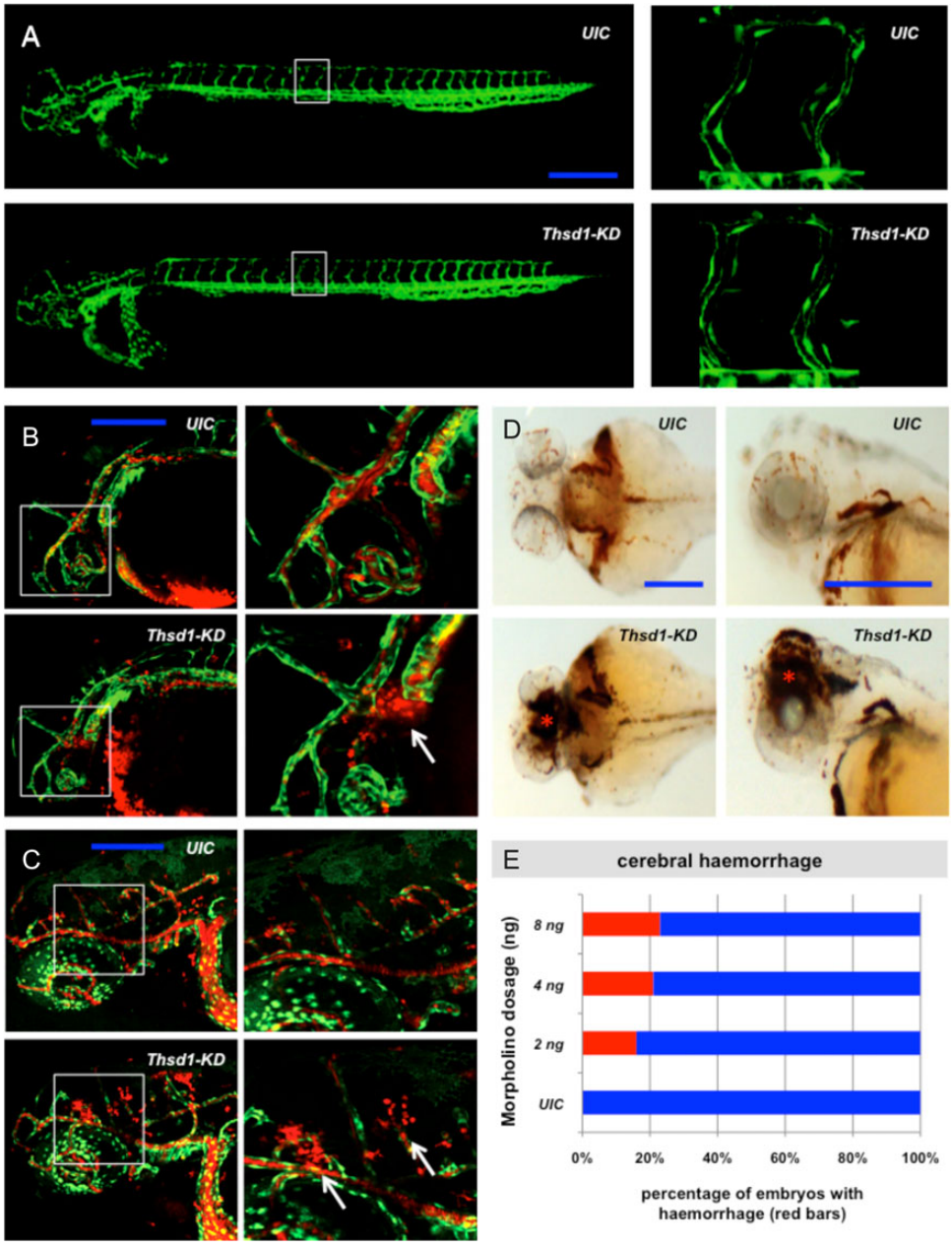


**Figure 2** Morpholino-induced knockdown of *thsd1* in zebrafish results in cerebral haemorrhages without affecting vascular growth. (*A*) Tg(fli1:eGFP)$^{y1}$ embryos at 26 hpf, lateral view, anterior to the left. Scale bar = 200 μm. No apparent morphological abnormalities in the trunk or cerebral vasculature were observed between *thsd1* targeting morpholino-injected (*thsd1*-KD) embryos and uninjected controls (UIC). Right-hand panel shows high magnification images of intersegmental outgrowth in the trunk region. Tg(kdrl:eGFP x gata1:dsRed)$^{y1}$ *thsd1*-KD embryos around (*B*) 28 hpf (Scale bar = 200 μm) and (*C*) 2 dpf (Scale bar = 100 μm), lateral view, anterior to the left. ECs (green) and erythrocytes (red). Right-hand panel shows high magnification images of the head region. Haemorrhages were detected in the head region (white arrow). (*D*) *o*-Dianisidine stained embryos around 28 hpf (Scale bar = 200 μm), top view (left) lateral view (right), anterior to the left. Areas of accumulated blood (red asterisk) in the head region were observed in *thsd1*-KD embryos. (*E*) Morpholino dose–response increase in the percentage of zebrafish with the cerebral haemorrhage phenotype (red bar) vs. the wild-type phenotype (no cerebral haemorrhaging, blue bar). ($n$ = 195 larvae in total).

## 3.4 *Thsd1* knockdown in the developing retinal vasculature of neonatal mice promotes vascular haemorrhages

In mice, vascularization of the retina takes place directly after birth, providing a 14-day time window to study the function of genes that are involved in angiogenesis in a non-embryonic setting. Here we used this neonatal retina vascularization model to study *Thsd1* following siRNA modulation of *Thsd1* expression. To determine the optimal moment of *Thsd1* knockdown, endogenous *Thsd1* mRNA expression in the murine retina during postnatal development was assessed by qPCR analysis. *Thsd1* mRNA levels were adjusted to CD31 mRNA

levels to compensate for changes in percentage of ECs during vascular expansion. *Thsd1* expression was observed from 3 to 15 days post-partum in the murine retinas (*Figure 3A*). Therefore, *Thsd1* knockdown was induced in the first week of retinal vascular development by intra-ocular injection of a siRNA pool composed of four different *Thsd1* targeting siRNA sequences (*Thsd1-KD*) in 2-day-old wild-type C57BL/6J mouse pups and compared with controls injected with a scrambled non-targeting siRNA pool (sham). Efficient knockdown of *Thsd1* was observed 2 days after intraocular injection (see Supplementary material online, *Figure S2A*). More specifically, endogenous *Thsd1* expression was significant down-regulated after siRNA targeting of *Thsd1* in the retinal endothelial cell population (PECAM1+) compared with the PECAM1+ endothelial cell population obtained from retinas injected with the non-targeting siRNA pool, as shown by qPCR after magnetic bead isolation of PECAM1+ cells in collagenase-digested retina samples (see Supplementary material online, *Figure S2B* and *C*). Furthermore, the non-endothelial cell population (PECAM-) showed far lower endogenous expression levels of *Thsd1* compared with the PECAM1+ population, and no significant down-regulation of *Thsd1* was detected in PECAM− cells derived from *Thsd1*-KD retinas.

Quantification of the vascular network after visualization of ECs by isolectin GS-$IB_4$ staining showed no difference between *Thsd1-KD* and sham-injected eyes 5 days after intraocular injection (*Figure 3B–E*). However, double staining of retinas with isolectin GS-$IB_4$ (ECs in green) and TER-119 antibody (detecting erythrocytes in red) showed a higher frequency and larger areas of haemorrhaging in the *Thsd1-KD*-injected eyes, whereas retinal haemorrhaging was hardly observed in sham-injected controls (*Figure 3F* and *G*). Thus, like in the developing

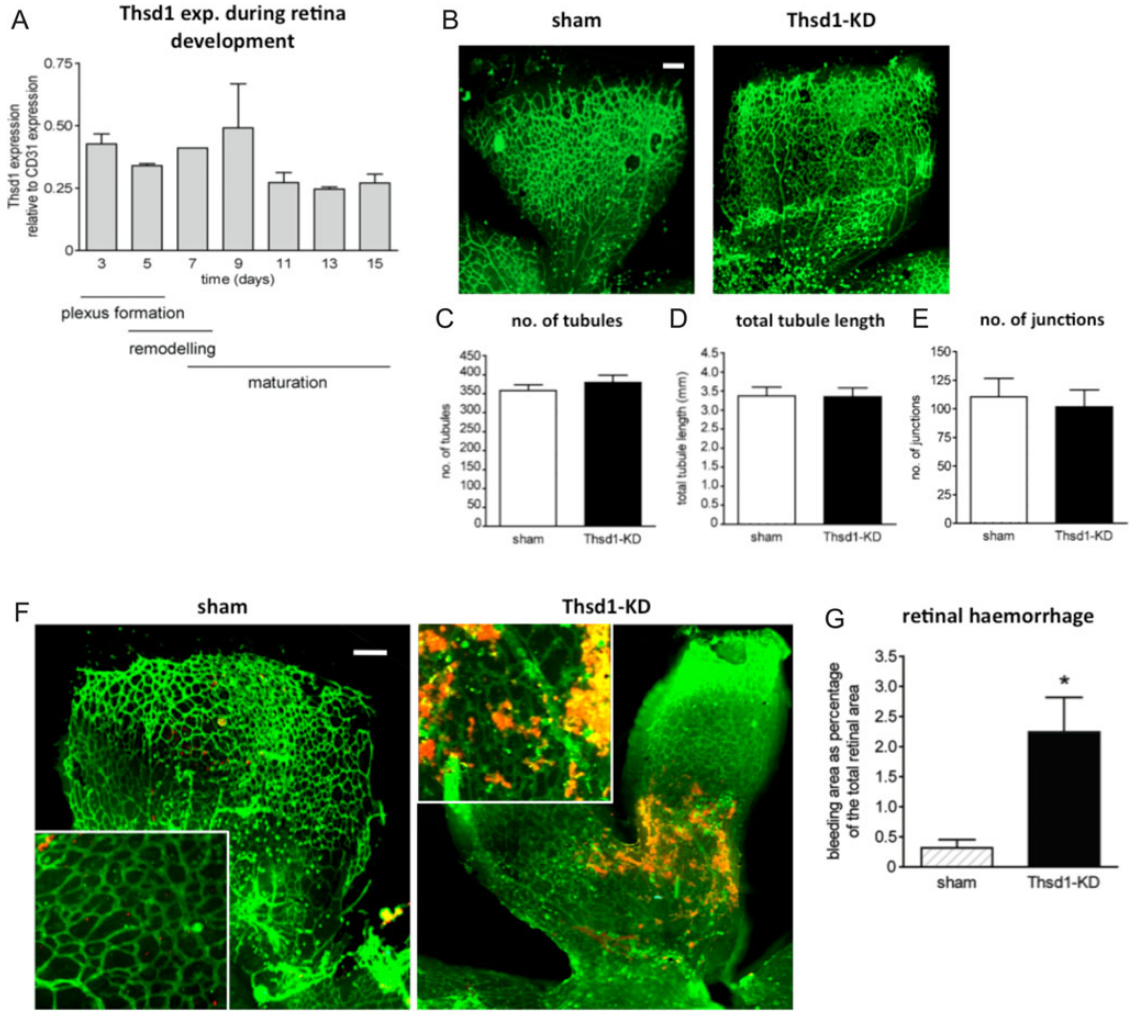


**Figure 3** *Thsd1* depletion during murine retinal vascular development results in vascular haemorrhaging without affecting vascular growth. (*A*) Endogenous expression level of *Thsd1* in the developing retinal vasculature of neonatal mice from 3 to 15 days after birth relative to CD31 expression ($n = 3$; mean ± SEM). *Thsd1* is highly expressed from Day 3 to 9, which coincides with the period of plexus formation and vascular remodelling. (*B*) Retinas stained with isolectin GS-$IB_4$ for detection of ECs (representatives are shown from each group, $n = 5$; Scale bar = 300 μm). Quantification of the vascular network showed no morphological defects after *Thsd1* knockdown (*Thsd1*-KD) regarding (*C*) number of tubules, (*D*) total tubule length, and (*E*) number of junctions. Double staining of retinas with isolectin GS-$IB_4$ (ECs green) and TER-119 (erythrocytes red) showed (*F*) significantly larger areas of vascular haemorrhaging in the *THSD1*-KD group. Inserted panels show high magnification details of the micrographs. (*G*) Quantification of retinal haemorrhage with the bleeding area expressed as percentage of the total retinal area in *Thsd1*-KD vs. sham retinas ($n = 10$; mean ± SEM). *$P < 0.05$ (Student's *t*-test), scale bar = 300 μm.

zebrafish, loss of *Thsd1* expression in the murine retinal vasculature had no effect on vascular growth, but induced high susceptibility to vascular haemorrhaging.

*THSD1* is expressed in advanced human atherosclerotic lesions with neovascular intraplaque haemorrhaging and increased plaque vulnerability

Intimal neovascular growth with compromised vascular integrity is an important contributor to atherosclerotic lesion destabilization. We investigated the role of *THSD1* in the pathophysiology of the compromised neovasculature in advanced atherosclerotic lesions. Ten human atherosclerotic plaques were obtained from patients with symptomatic carotid artery disease and were divided into a group of 5 stable lesions and a group of 5 advanced vulnerable plaques with pathological evidence of intraplaque haemorrhaging. *THSD1* and *CD31* expression was determined by immunohistological staining (see Supplementary material online, *Figure S3A*). THSD1 signal was co-localized with CD31+ ECs in vulnerable plaques with intraplaque haemorrhaging, whereas in stable plaques, *THSD1* expression by ECs was not detected (see Supplementary material online, *Figure S3A*). *THSD1* expression in human endothelial cells ( s) *in vitro* could be decreased by two prominent pro-atherogenic stimuli, low oxygen (3% $O_2$) and TNFα (see Supplementary material online, *Figure S3B* and *C*), but was significantly up-regulated by the anti-atherogenic stimulus IL10 (see Supplementary material online, *Figure S3D*). *THSD1* expression appears to be sensitive to distinct transition points in TNFα and IL10 concentrations. These findings point towards a potential role for *THSD1* in endothelial barrier dysfunction in advanced atherosclerotic lesions vulnerable to rupture.

## 3.5 *Thsd1* attenuates intraplaque haemorrhage and plaque destabilization without affecting neovascular growth

Findings in our zebrafish and murine retina models indicate that *Thsd1* is a beneficial factor for maintaining endothelial barrier function. We hypothesize that *Thsd1* expression in vulnerable plaque is part of an endogenous protective mechanism to counteract loss of endothelial integrity. The effect of *Thsd1* overexpression was assessed in our well-validated murine ApoE-knockout model in which we induced growth of carotid atherosclerotic lesions by shear stress alteration by implanting a tapered perivascular cast around the carotid artery.[11,12] In this murine model, a vulnerable plaque-like lesion develops in the low shear stimulated up-stream carotid region from the cast, whereas a stable plaque develops in the oscillatory shear stimulated downstream region from the cast.[11,12] Endogenous *Thsd1* expression in the normal carotid arteries of non-treated ApoE-knockout mice was already markedly increased in response to 1 week of feeding a high cholesterol, high fat diet (see Supplementary material online, *Figure S4B*). In line with the findings in the human samples, endogenous *Thsd1* mRNA level was significantly increased in the vulnerable plaque compared with the stable lesions derived from the murine cast model [$n = 5$; $^*P < 0.05$; Mann–Whitney *U* test; $23.0 \pm 1.14$ vs. $13.2 \pm 0.86$ (mean ± SEM); vulnerable vs. stable plaque, respectively, as determined by qPCR].

Peri-adventitial infection of an adenovirus expressing murine *Thsd1* (*adThsd1*) in the carotid artery resulted in a significant increase in *Thsd1* mRNA expression compared with infection with a sham virus (adsham) (see Supplementary material online, *Figure S4A*). Overexpression of *Thsd1* attenuated the vulnerable plaque phenotype at 9 weeks post shear stress-induced atherosclerosis induction: A 45% decrease in intimal accumulation of TER-119 erythrocytes was observed (*Figure 4A* and *B*). In addition, dextran-FITC extravasation was significantly reduced in the plaque intima (*Figure 4C*) and surrounding vasa vasorum of *adThsd1*-treated murine carotid arteries compared with adsham-treated controls (*Figure 4D*). These effects were independent of intimal neovascular growth, as no change in the number of CD31-positive cells was detected (*Figure 4E* and *F*).

Coincided with improved neovascular integrity, a 36% reduction in intraplaque macrophage accumulation in the *adThsd1* group was observed (*Figure 4G* and *H*), whereas intraplaque lipid accumulation remained unaffected (*Figure 4I* and *J*). This reduction in intraplaque macrophages did not affect lesion size as measured by intima/media ratio (*Figure 4K* and *L*). However, necrotic core area was significantly decreased in the *adThds1* group (*Figure 4K* and *M*). Together, these data demonstrate that *Thsd1* overexpression restores compromised endothelial barrier function of the intimal microvasculature in murine vulnerable plaque-like lesions.

## 3.6 *THSD1* controls endothelial barrier function *in vitro*

Next we conducted *in vitro* assays to further define the mechanistic function of THSD1 in vascular cells. The expression level of *THSD1* was evaluated in different cell types. On comparing HUVEC, pericyte, VSMC, and fibroblast, the highest mRNA expression level of *THSD1* was observed in HUVECs (*Figure 5A*). In line with previous *in vivo* findings, siRNA-mediated knockdown of *THSD1* (*THSD1-KD*) in HUVECs did not affect network formation in a standard 2D Matrigel assay compared with cultures transfected with equimolar of non-targeting sham siRNA (sham) (*Figure 5B–E*). Adequate knockdown of the target gene was validated on both mRNA and protein level (see Supplementary material online, *Figure S5A* and *B*), and did not affect the expression of other genes that contain the TSP1 domain, such as Thrombospondin 1 (see Supplementary material online, *Figure S5C*).

A transwell permeability assay that measures HRP passage was carried out to determine the effect of *THSD1* on endothelial barrier function in HUVECs. In line with our *in vivo* findings, endothelial barrier function was significantly decreased in *THSD1* knockdown HUVECs as shown by increased permeability for HRP (*Figure 5F*). Evaluation of endothelial barrier function by ECIS (Electric Cell-substrate Impedance Sensing) also demonstrated that *THSD1* silencing in HUVEC monolayers impeded the build-up of endothelial electric resistance compared with sham treated cells (*Figure 5G*). These data indicate that endothelial barrier function in *THSD1* knockdown endothelial cells is compromised at the cell junction level.

## 3.7 *THSD1* mediates cell-to-cell interaction via activation of Rac1

Rac1 is an important mediator of endothelial barrier function as it enforces cell-to-cell and cell-ECM interaction via regulation of the actin cytoskeleton.[15,16] Here we evaluated the impact of *THSD1* knockdown on Rac1 activation via the FAK-PI3K pathway (*Figure 6A–G*). Knockdown of *THSD1* significantly decreased total FAK protein levels and FAK phosphorylation at the Y397 site (*Figure 6A* and *B*) without affecting the FAK-phospho/total FAK ratio ($^*P < 0.05$, sham vs. *THSD1*-KD). PI3K phosphorylation at position Y508 was significantly diminished without affecting total PI3K protein levels (*Figure 6C* and *D*). Similarly, the PI3K-phospho/total PI3K ratio was decreased ($^*P < 0.05$, sham vs. *THSD1*-KD). Further downstream, *THSD1*

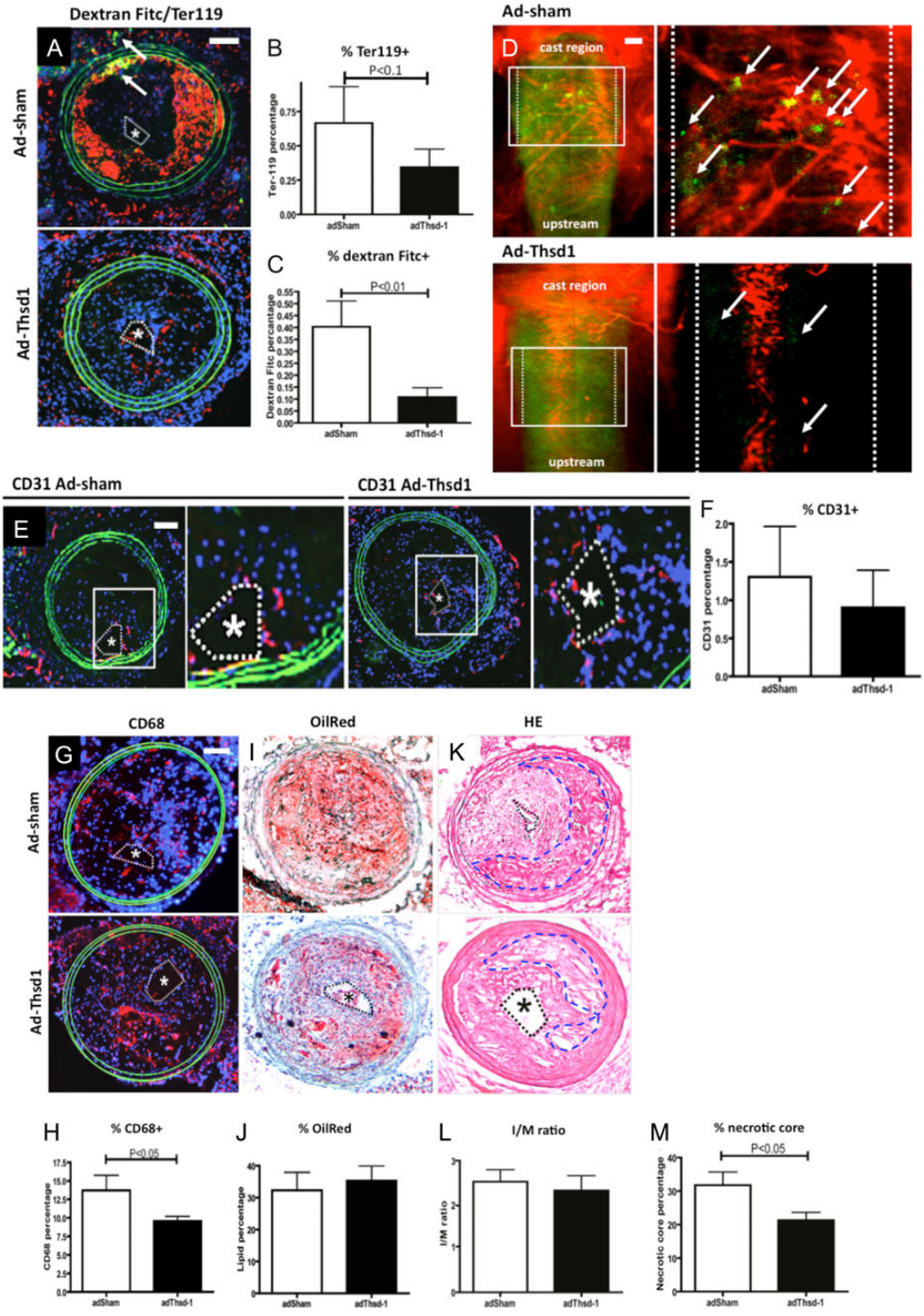


**Figure 4** Overexpression of *Thsd1* attenuates intraplaque haemorrhaging and stabilizes plaque vulnerability in murine vulnerable plaque-like lesions. (*A*) Cryosections of adsham and Ad*Thsd1*-treated ApoE-knockout mice infused with dextran-FITC through the left heart ventricle during sacrifice with carotid plaque lesions stained for TER-119 (red) and visible dextran-FITC perivascular leakage in the intima and adventitia (white arrows). (*B*) Quantification of the percentage of TER-119+ area per carotid plaque cross-section. (*C*) Percentage of dextran-FITC+ area per carotid plaque cross-section. (*D*) Whole mount samples with adventitial vasculature stained for isolectin GS-$IB_4$ (ECs, red) with detection of dextran-FITC perivascular leakage (green, indicated by arrows) in the upstream (atherosclerotic) carotid region from the shear stress device. Dotted lines indicate vessel boundaries (representative micrograph of $n = 6$). Sections of adsham and Ad*Thsd1*-treated ApoE-knockout mice with carotid plaque lesions stained for (*E*) CD31+ endothelial cells, (*G*) CD68+ macrophages, (*I*) lipids, and (*K*) haematoxylin/eosin. Quantification of the percentage of (*F*) CD31+ area, (*H*) CD68+ area, (*J*) OilRed O+ area, (*L*) the intima/media ratio, and (*M*) necrotic core area (indicated by blue dotted lines in *K*) per cross-section. For all cross-sections, lumen areas are indicated by black dotted lines marked by an asterisk. For *A*, *E*, and *G*, elastin (autofluorescent green), dextran-FITC (green), DAPI (blue), TER-119, CD31 and CD68 (red) ($n = 10$; mean ± SEM; *P*-values based on Student's *t*-test). Scale bar = 200 μm.

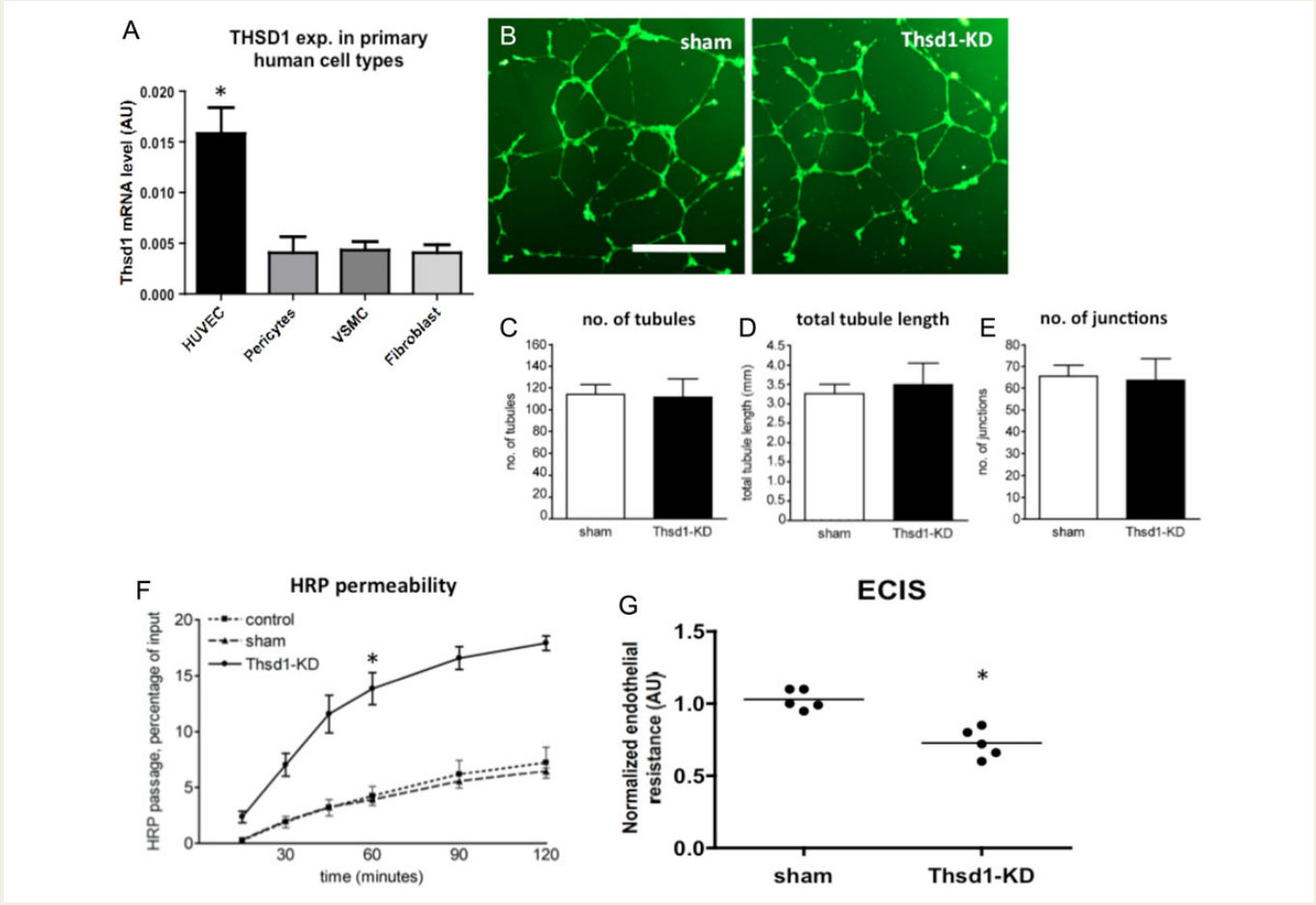


**Figure 5** *THSD1* knockdown in cultured endothelial cells impairs endothelial barrier function. (*A*) *THSD1* was highly expressed in HUVEC vs. pericyte, VSMC, and fibroblast, as demonstrated by qPCR analysis. ($n = 6$); mean ± SEM normalized to housekeeping gene and indicated in arbitrary units (AU) *$P < 0.05$ vs. all; Kruskal–Wallis test followed by Dunn's multiple comparison test. (*B*) Assessment of network formation capacity of HUVECs transfected with *THSD1* targeting siRNA (*THSD1*-KD) compared with HUVECs treated with non-targeting siRNA (sham) in a 2D Matrigel experiment. HUVECs were stained with Calcein-AM. Scale bar = 100 μm. Quantification of the vascular network showed no morphological defects after *THSD1-KD* regarding (*C*) number of tubules, (*D*) total tubule length, and (*E*) number of junctions ($n = 4$; mean ± SEM; Mann–Whitney *U* test). (*F*) Measurement of endothelial barrier function *in vitro*. Passage of horseradish peroxidase (HRP) over a confluent monolayer of HUVECs during thrombin (1 U/mL) stimulation for the different conditions over time. *$P < 0.05$ vs. control and si-sham; Bonferroni *post hoc* test of repeated-measures ANOVA. ($n = 3$; mean ± SEM) (*G*) ECIS measurement over a confluent monolayer of HUVECs shows a delay in electric resistance build-up after *THSD1* knockdown at 45 h post seeding. *$P < 0.05$ vs. HUVECs treated with si-sham; Mann–Whitney *U* test ($n = 5$; mean ± SEM in arbitrary units (AU) after normalization for each well to the starting level of resistance measured at 4 h post seeding).

silencing inhibited PI3K-mediated Rac1 activation, while total Rac1 protein levels remained unaffected (*Figure 6E* and *F*). These data indicate that *THSD1* acts through regulation of total FAK protein levels and by affecting PI3K phosphorylation levels.

To validate whether this *THSD1*-induced modulation of Rac1 activity is indeed a critical factor in the THSD1-mediated mechanisms, *THSD1*-silenced HUVECs were treated with a pharmaceutical activator for Rac1 in the *in vitro* transwell permeability assay. Rac1 stimulation decreased endothelial permeability after *THSD1* knockdown (see Supplementary material online, *Figure S6A*), confirming that loss of endothelial barrier function, as induced by *THSD1* knockdown, was indeed mediated via Rac1 inhibition. For further validation, a phenotype rescue experiment was carried out in the murine retina model: *Thsd1* was silenced in combination with treatment with the Rac1 activator and compared with controls with intra-ocular injection of *Thsd1* targeting siRNAs only. Rac1 activation reversed the effects of *Thsd1* silencing with a clear reduction in vascular haemorrhaging (*$P < 0.05$; Mann–Whitney *U* test; 2.6 ± 0.18 vs. 0.91 ± 0.18 (mean ± SEM); *Thsd1*-KD vs. *Thsd1*-KD + Rac1 activator respectively; see Supplementary material online, *Figure S6B*).

To study the Rac1-mediated function of *THSD1* in actin dynamics, cell spreading, and actin filament distribution was evaluated at different time points after cell seeding (*Figure 6H* and *I*). Quantification and stratification of actin cytoskeleton surface per cell showed that *THSD1* knockdown induced a trend towards decrease in the number of cells with a large actin cytoskeleton surface (>1500 $nm^2$) at 30 min post seeding compared with sham transfected controls (*Figure 6I*). This decline in spreading efficiency was associated with a defect in ECM interaction: Visualization of focal adhesion sites showed a significant decline of Paxillin and Vinculin capping at actin stress fibre ends of *THSD1*-silenced cells (see Supplementary material online, *Figure S7A–D*).

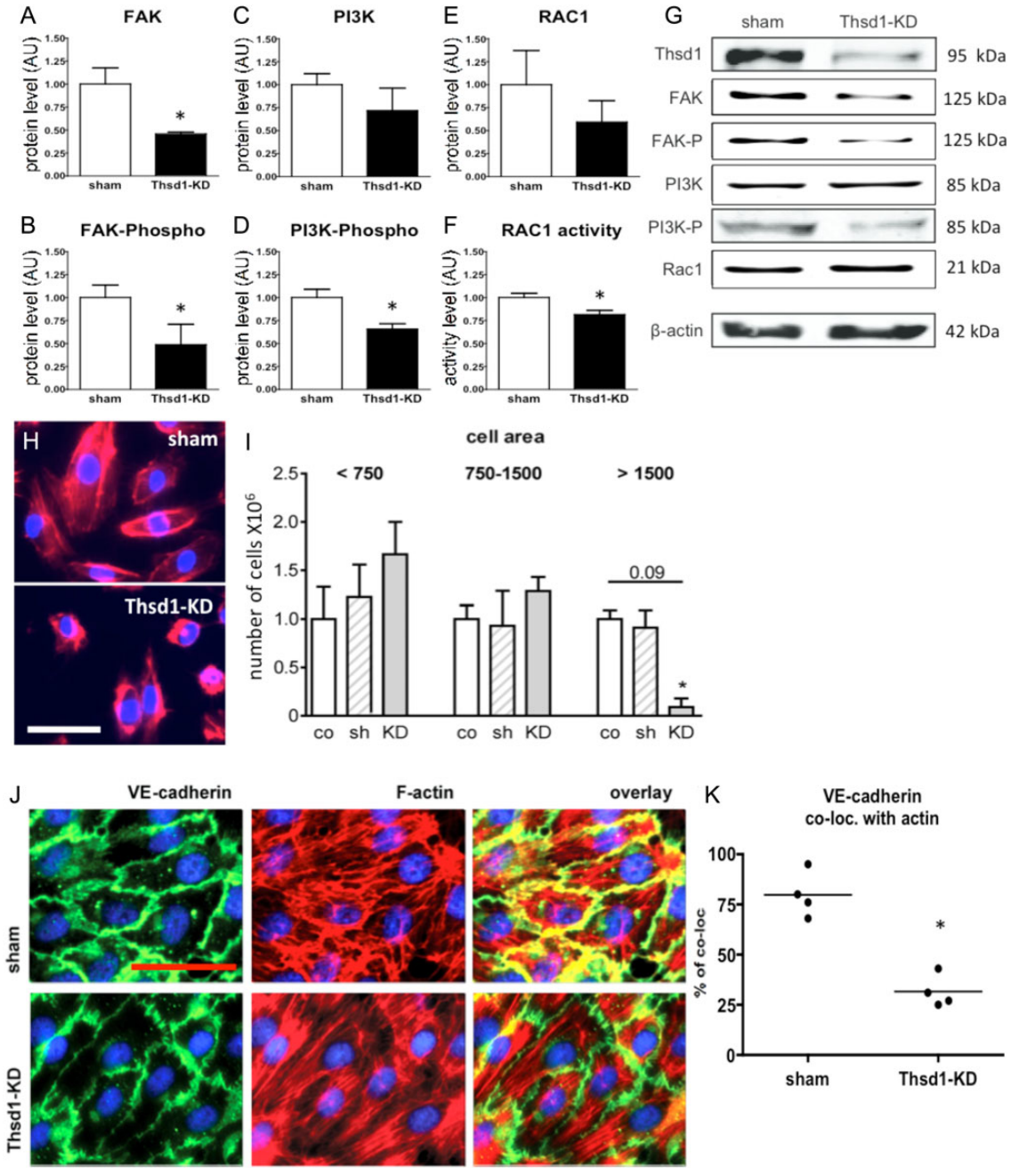


**Figure 6** *THSD1* induces actin cytoskeleton modulation via Rac1 activation. Western blot analysis of (*A*) FAK, (*B*) FAK-PhosphoY397 (*C*) PI3K, (*D*) PI3K-PhosphoY508, and (*E*) Rac1 protein levels normalized to ß-actin in *THSD1-KD* or sham conditions. (*F*) Rac1 GTPase activity levels as measured by G-lisa assays in sham and *THSD1-KD* conditions. (*G*) Representative western blot results for the assessed proteins with ß-actin loading control. [for *A*–*F*; $n = 4$; mean ± SEM in arbitrary units (AU)] *$P < 0.05$ vs. sham; Mann–Whitney *U* test. *THSD1-KD* impairs actin cytoskeleton dynamics during cell spreading. Actin mobility was assessed in a cell-spreading assay. (*H*) Thirty minutes after cell seeding, *THSD1-KD* showed a delay in actin cytoskeleton spreading. F-actin (red) and nuclei (blue). Scale bar = 50 μm. (*I*) Quantification of the actin cytoskeleton surface area per cell showed a decrease in the number of cells with a large actin cytoskeleton surface area (>1500 $nm^2$) after *THSD1* knockdown ($n = 3$; mean ± SEM). *$P < 0.1$ vs. sham or non-transfected control; Kruskal–Wallis test followed by Dunn's multiple comparison test. *THSD1-KD* impairs VE-cadherin-actin cytoskeleton colocalization. (*J*) *THSD1-KD* in HUVECs reduced co-localization of VE-cadherin with the actin cytoskeleton as demonstrated by immunofluorescent staining. VE-cadherin (green), F-actin (red), co-localized area (yellow), and nuclei (blue). (*K*) Quantification of the percentage of VE-cadherin that is co-localized with actin filaments ($n = 4$; mean ± SEM). Scale bar = 50 μm. *$P < 0.05$ vs. sham; Mann–Whitney *U* test.

Loss of association between VE-cadherin and the actin cytoskeleton at adherens junction sites promotes endothelial and thus vascular permeability.[3] The effect of *THSD1* knockdown on VE-cadherin-actin cytoskeleton association was assessed in confluent HUVEC monolayers. Knockdown of *THSD1* in HUVECs reduced co-localization of VE-cadherin with the actin cytoskeleton (*Figure 6J* and *K*). Taken together, these data suggest that

*THSD1* modulates cell-to-cell interaction via a signalling mechanism that involves FAK-PI3K during Rac1-mediated regulation of the endothelial actin cytoskeleton.

# 4. Discussion

In this study, we identified *THSD1* as a new potent regulator of endothelial barrier function during physiological vascular development using *in vivo* zebrafish and mouse vascular growth models. In both embryonic zebrafish and postnatal murine pups, *Thsd1* silencing affected vascular integrity during angiogenesis, whereas vascular expansion remained effective. Mechanistically, our experiments with *THSD1*-silenced HUVECs in HRP and ECIS assays have demonstrated that endothelial barrier function was affected. Several mutant zebrafish lines have been described to display a similar vascular phenotype with hallmark haemorrhaging in the cranial region, including germ-line mutations in heg1, ccm1, ccm2, and ccm3.[14,17,18] Like *thsd1*, these genes appear to be involved in Rac1 activation and RhoA degradation.[19]

Activation of the small GTPase Rac1 in endothelial cells is a crucial factor in support of cell junction integrity and preservation of the endothelial barrier during vascular quiescence.[20–22] Rac1 activation promotes cell spreading by decreasing cell contractility via actomyosin suppression and by counteracting RhoA-induced actin stress fibre formation. Activation of Rac1 has also been reported to preserve VE-cadherin adherens junctions.[20,21,23] In contrast, inhibition of Rac1 by RhoA and Src through ß-integrin signalling induces actin stress fibre formation and disruption of VE-cadherin junctions.[22] We showed in this study that *THSD1* knockdown diminished Rac1 activity. This was coincided with a reduction in Rac1 downstream responses, including a decrease in actin cytoskeleton morphological adaptation during cell spreading in cell adhesion assays. Rac1-modulated cell spreading is part of the Rac1 and Cdc42 regulatory pathway to spatially control the formation of filopodia and lamellipodia, which favours the formation of barrier improvement.[2] Thus, THSD1 knockdown appears to directly inhibit this Rac1-mediated barrier stabilization pathway. Further downstream, decrease in Rac1 activation would lead to loss of actomyosin suppression and stress fibre formation, inducing endothelial cell contraction, and causing the formation of intercellular gaps and disruption of VE-cadherin junctions. In thrombin studies using confluent monolayers of HUVECs we showed that knockdown of *THSD1* significantly reduced co-localization of VE-cadherin with actin filaments, indicative of loss of functional adherens junctions.[3] Anchorage of VE-cadherin proteins to the actin cytoskeleton via a complex of adherens junction proteins plays a crucial role in controlling endothelial morphology and permeability.[2,24] However, the exact molecular basis of this regulation remains to be further clarified. Together the findings from our *in vitro* mechanistic studies demonstrate that *THSD1* regulates endothelial barrier function by Rac1 activation and the subsequent preservation of cell-to-cell junctions and cell-to-ECM focal adhesions via actin cytoskeleton dynamics. In our studies, *Thsd1* expression in the developing murine embryo was highest in Flk1-positive angioblasts compared with Flk1-negative cells, while whole mount *in situ* hybridization in developing zebrafish larvae validated the predominant vascular expression of *Thds1*. *THSD1* may thus be regarded as an endothelial regulator of Rac1 activity that plays a prominent role in the preservation of endothelial barrier function, in particular during angiogenesis.

The current study has also highlighted the therapeutic potential of THSD1 in treatment of cardiovascular disease. Neovascular growth driven by intimal hypoxia often results in the formation of immature and fragile microvessels in advanced atherosclerotic lesions.[25] These intraplaque microvessels display extravasation of leucocytes and erythrocytes, which leads to intimal inflammation, expansion of the necrotic core, and intraplaque haemorrhaging. Recent evidence indicates that intraplaque haemorrhaging plays an important role in lesion progression towards a vulnerable plaque.[26,27] Restoration of endothelial integrity in compromised intraplaque vessels might prevent plaque destabilization and vulnerable plaque formation.[8] Assessment of human carotid endarterectomy specimens demonstrated *THSD1* expression by intimal microvascular ECs in advanced vulnerable lesions with intraplaque haemorrhaging. *THSD1* expression was absent in stable plaques. Furthermore, Thsd1 expression was significantly up-regulated in the vulnerable plaques compared with stable lesions in our murine vulnerable plaque model. These findings seem counterintuitive and difficult to integrate with the notion that *THSD1* is endothelial barrier protective. However, the findings of our *Thsd1* gain-of-function studies in our murine vulnerable plaque model further provide evidence that *Thsd1* promotes vascular integrity: Intraplaque haemorrhaging was decreased in advanced lesions in response to *Thsd1* overexpression. THSD1 expression in adults could be dependent on activation by micro-environmental factors. In support of this hypothesis, *THSD1* expression was induced by IL10, a secreted factor with plaque stabilizing properties and increased expressed in unstable lesions.[28,29]

Furthermore, THSD1 may be involved in regulating monocyte extravasation via activation of adhesion molecules and release of chemotactic cytokines. How different angiogenic modulators influence THSD1 function during vascular expansion and the effects of THSD1 on interaction between circulatory immune cells and the endothelium in adult condition remain to be further investigated.

In conclusion, in the current study, we have identified THSD1 as a new regulator of vascular integrity in vascular development and advanced vascular disease. To our knowledge, our findings are the first to report on the biological function of THSD1 in ECs during normal embryonic and early postnatal blood vessel formation. In advanced atherosclerotic lesions, overexpression of THSD1 can restore endothelial barrier function in the intraplaque neovasculature and protect the plaque from extensive haemorrhaging and further disease progression. In the light of our findings of the basic and pathophysiological function of *THSD1*, the gene may be considered to be an interesting target for the development of novel diagnostics and therapeutics in the treatment of atherosclerosis and other vascular-related diseases for which the pathophysiology involves loss of (micro)vascular integrity during angiogenic growth.

# Supplementary material

Supplementary material is available at *Cardiovascular Research* online.

**Conflict of interest:** none declared.

## Funding

This work was funded by grants from the Dutch Heart Foundation (2011T072 to G.P.v.N.A.), the Dutch Organization for Scientific Research (grant nr. 91776325 to H.J.D., and grant nr. 91696061 and grant nr. 91714302 to C.C.), the EMC fellowship grant [C.C.] and UMCU RM fellowship grant [C.C.].

## References


1. Klaassen I, Van Noorden CJ, Schlingemann RO. Molecular basis of the inner blood-retinal barrier and its breakdown in diabetic macular edema and other pathological conditions. *Prog Retin Eye Res* 2013;**34**:19–48.
2. Giannotta M, Trani M, Dejana E. VE-cadherin and endothelial adherens junctions: active guardians of vascular integrity. *Dev Cell* 2013;**26**:441–454.
3. Kim SH, Cho YR, Kim HJ, Oh JS, Ahn EK, Ko HJ, Hwang BJ, Lee SJ, Cho Y, Kim YK, Stetler-Stevenson WG, Seo DW. Antagonism of VEGF-A-induced increase in vascular permeability by an integrin alpha3beta1-Shp-1-cAMP/PKA pathway. *Blood* 2012;**120**:4892–4902.
4. Tian X, Tian Y, Sarich N, Wu T, Birukova AA. Novel role of stathmin in microtubule-dependent control of endothelial permeability. *FASEB J* 2012;**26**:3862–3874.
5. Spindler V, Schlegel N, Waschke J. Role of GTPases in control of microvascular permeability. *Cardiovasc Res* 2010;**87**:243–253.
6. Broman MT, Mehta D, Malik AB. Cdc42 regulates the restoration of endothelial adherens junctions and permeability. *Trends Cardiovasc Med* 2007;**17**:151–156.
7. Daneshjou N, Sieracki N, van Nieuw Amerongen GP, Conway DE, Schwartz MA, Komarova YA, Malik AB. Rac1 functions as a reversible tension modulator to stabilize VE-cadherin trans-interaction. *J Cell Biol* 2015;**209**:181.
8. Jain RK, Finn AV, Kolodgie FD, Gold HK, Virmani R. Antiangiogenic therapy for normalization of atherosclerotic plaque vasculature: a potential strategy for plaque stabilization. *Nat Clin Pract Cardiovasc Med* 2007;**4**:491–502.
9. Sluimer JC, Daemen MJ. Novel concepts in atherogenesis: angiogenesis and hypoxia in atherosclerosis. *J Pathol* 2009;**218**:7–29.
10. Takayanagi S, Hiroyama T, Yamazaki S, Nakajima T, Morita Y, Usui J, Eto K, Motohashi T, Shiomi K, Keino-Masu K, Masu M, Oike Y, Mori S, Yoshida N, Iwama A, Nakauchi H. Genetic marking of hematopoietic stem and endothelial cells: identification of the Tmtsp gene encoding a novel cell surface protein with the thrombospondin-1 domain. *Blood* 2006;**107**:4317–4325.
11. Cheng C, Tempel D, van Haperen R, de Boer HC, Segers D, Huisman M, van Zonneveld AJ, Leenen PJ, van der Steen A, Serruys PW, de Crom R, Krams R. Shear stress-induced changes in atherosclerotic plaque composition are modulated by chemokines. *J Clin Invest* 2007;**117**:616–626.
12. Cheng C, Noordeloos AM, Jeney V, Soares MP, Moll F, Pasterkamp G, Serruys PW, Duckers HJ. Heme oxygenase 1 determines atherosclerotic lesion progression into a vulnerable plaque. *Circulation* 2009;**119**:3017–3027.
13. Gjini E, Hekking LH, Kuchler A, Saharinen P, Wienholds E, Post JA, Alitalo K, Schulte-Merker S. Zebrafish Tie-2 shares a redundant role with Tie-1 in heart development and regulates vessel integrity. *Dis Model Mech* 2011;**4**:57–66.
14. Kleaveland B, Zheng X, Liu JJ, Blum Y, Tung JJ, Zou Z, Sweeney SM, Chen M, Guo L, Lu MM, Zhou D, Kitajewski J, Affolter M, Ginsberg MH, Kahn ML. Regulation of cardiovascular development and integrity by the heart of glass-cerebral cavernous malformation protein pathway. *Nat Med* 2009;**15**:169–176.
15. Huveneers S, Oldenburg J, Spanjaard E, van der Krogt G, Grigoriev I, Akhmanova A, Rehmann H, de Rooij J. Vinculin associates with endothelial VE-cadherin junctions to control force-dependent remodeling. *J Cell Biol* 2012;**196**:641–652.
16. Kraemer A, Goodwin M, Verma S, Yap AS, Ali RG. Rac is a dominant regulator of cadherin-directed actin assembly that is activated by adhesive ligation independently of Tiam1. *Am J Physiol Cell Physiol* 2007;**292**:C1061–9.
17. Voss K, Stahl S, Hogan BM, Reinders J, Schleider E, Schulte-Merker S, Felbor U. Functional analyses of human and zebrafish 18-amino acid in-frame deletion pave the way for domain mapping of the cerebral cavernous malformation 3 protein. *Hum Mutat* 2009;**30**:1003–1011.
18. Stainier DY, Fouquet B, Chen JN, Warren KS, Weinstein BM, Meiler SE, Mohideen MA, Neuhauss SC, Solnica-Krezel L, Schier AF, Zwartkruis F, Stemple DL, Malicki J, Driever W, Fishman MC. Mutations affecting the formation and function of the cardiovascular system in the zebrafish embryo. *Development* 1996;**123**:285–292.
19. Faurobert E, Albiges-Rizo C. Recent insights into cerebral cavernous malformations: a complex jigsaw puzzle under construction. *FEBS J* 2010;**277**:1084–1096.
20. Waschke J, Burger S, Curry FR, Drenckhahn D, Adamson RH. Activation of Rac-1 and Cdc42 stabilizes the microvascular endothelial barrier. *Histochem Cell Biol* 2006;**125**:397–406.
21. Wojciak-Stothard B, Potempa S, Eichholtz T, Ridley AJ. Rho and Rac but not Cdc42 regulate endothelial cell permeability. *J Cell Sci* 2001;**114**(Pt 7):1343–1355.
22. Davis GE, Senger DR. Endothelial extracellular matrix: biosynthesis, remodeling, and functions during vascular morphogenesis and neovessel stabilization. *Circ Res* 2005;**97**:1093–1107.
23. Good DJ, Polverini PJ, Rastinejad F, Le Beau MM, Lemons RS, Frazier WA, Bouck NP. A tumor suppressor-dependent inhibitor of angiogenesis is immunologically and functionally indistinguishable from a fragment of thrombospondin. *Proc Natl Acad Sci USA* 1990;**87**:6624–6628.
24. Dejana E, Orsenigo F, Lampugnani MG. The role of adherens junctions and VE-cadherin in the control of vascular permeability. *J Cell Sci* 2008;**121**(Pt 13):2115–2122.
25. Moreno PR, Purushothaman KR, Sirol M, Levy AP, Fuster V. Neovascularization in human atherosclerosis. *Circulation* 2006;**113**:2245–2252.
26. Kolodgie FD, Gold HK, Burke AP, Fowler DR, Kruth HS, Weber DK, Farb A, Guerrero LJ, Hayase M, Kutys R, Narula J, Finn AV, Virmani R. Intraplaque hemorrhage and progression of coronary atheroma. *N Engl J Med* 2003;**349**:2316–2325.
27. Michel JB, Virmani R, Arbustini E, Pasterkamp G. Intraplaque haemorrhages as the trigger of plaque vulnerability. *Eur Heart J* 2011;**32**:1977–1985, 1985a, 1985b, 1985c.
28. Mallat Z, Besnard S, Duriez M, Deleuze V, Emmanuel F, Bureau MF, Soubrier F, Esposito B, Duez H, Fievet C, Staels B, Duverger N, Scherman D, Tedgui A. Protective role of interleukin-10 in atherosclerosis. *Circ Res* 1999;**85**:e17–e24.
29. Nishihira K, Imamura T, Yamashita A, Hatakeyama K, Shibata Y, Nagatomo Y, Date H, Kita T, Eto T, Asada Y. Increased expression of interleukin-10 in unstable plaque obtained by directional coronary atherectomy. *Eur Heart J* 2006;**27**:1685–1689.